PLOS ONE

RESEARCH ARTICLE

Conditional KCa3.1-transgene induction in murine skin produces pruritic eczematous dermatitis with severe epidermal hyperplasia and hyperkeratosis

Javier Lozano-Gerona[1], Aida Oliván-Viguera[2], Pablo Delgado-Wicke[3], Vikrant Singh[4], Brandon M. Brown[4], Elena Tapia-Casellas[5], Esther Pueyo[2], Marta Sofía Valero[6], Ángel-Luis Garcia-Otín[1], Pilar Giraldo[7], Edgar Abarca-Lachen[8], Joaquín C. Surra[9], Jesús Osada[10], Kirk L. Hamilton[11], Siba P. Raychaudhuri[12], Miguel Marigil[13], Ángeles Juarranz[3,14], Heike Wulff[4], Hiroto Miura[15], Yolanda Gilaberte[16], Ralf Köhler[1,17]*

1 Instituto Aragonés de Ciencias de la Salud (IACS) y Instituto de Investigación Sanitaria (IIS) Aragón, Zaragoza, Spain, **2** Biosignal Interpretation and Computational Simulation (BSICoS), Aragón Institute of Engineering Research (I3A), Univ. of Zaragoza, Zaragoza, Spain, **3** Departamento de Biología, Facultad de Ciencias, UAM, Madrid, Spain, **4** Dept. of Pharmacology, University of California, Davis, CA, United States of America, **5** Scientific and Technical Service, Aragónese Center for Biomedical Research, Univ. of Zaragoza, Zaragoza, Spain, **6** Dept. of Pharmacology and Physiology, Univ. of Zaragoza, Huesca, Spain, **7** Spanish Foundation for the Study and Treatment of Gaucher Disease and other Lysosomal Disorders (FEETEG), Zaragoza, Spain, **8** Universidad San Jorge, Faculty of Health Sciences, Villanueva de Gállego, Spain, **9** Departamento de Producción Animal y Ciencia de los Alimentos, CIBER-obn, Univ. of Zaragoza, Zaragoza, Spain, **10** Departamento Bioquímica y Biología Molecular y Celular (CIBEROBN), Facultad de Veterinaria, Univ. of Zaragoza, Zaragoza, Spain, **11** Dept. of Physiology, School of Biomedical Sciences, Univ. of Otago, Dunedin, New Zealand, **12** Department of Medicine and Dermatology, School of Medicine UC Davis and VA Sacramento Medical Center University of California, Mather, California, United States of America, **13** Dept. of Pathology, Hospital San Jorge, Huesca, Spain, **14** Instituto Ramón y Cajal de Investigaciones Sanitarias (IRYCIS), Madrid, Spain, **15** Dept. of Physiology and Cell Biology, University of Nevada School of Medicine, Reno, NV, United States of America, **16** Dept. of Dermatology, Univ. Hospital Miguel Servet, IIS Aragón, Zaragoza, Spain, **17** Aragón Agency for Research and Development (ARAID), Zaragoza, Spain

* kohler@araid.es

OPEN ACCESS

Citation: Lozano-Gerona J, Oliván-Viguera A, Delgado-Wicke P, Singh V, Brown BM, Tapia-Casellas E, et al. (2020) Conditional KCa3.1-transgene induction in murine skin produces pruritic eczematous dermatitis with severe epidermal hyperplasia and hyperkeratosis. PLoS ONE 15(3): e0222619. https://doi.org/10.1371/journal.pone.0222619

Editor: Michel Simon, INSERM, FRANCE

Received: August 28, 2019

Accepted: February 13, 2020

Published: March 9, 2020

Data Availability Statement: All relevant data are within the manuscript and its Supporting Information files.

Funding: This work was supported by the Government of Aragón (DGA-METIC–consortium; B04_17R), FP7-PEOPLE-MC-CIG to RK, FIS-CB06/07/1036 to PG and RK, ERC-2014-StG-638284, DPI2016-75458-R, T39_17R to EP; FIS-PI16/02112 to ALGO; NHLBI-R01-HL080173, NCRR-P20-RR018751 to HM. JLG received a DGA-PhD

Abstract

Ion channels have recently attracted attention as potential mediators of skin disease. Here, we explored the consequences of genetically encoded induction of the cell volume-regulating Ca^{2+}-activated KCa3.1 channel (*Kcnn4*) for murine epidermal homeostasis. Doxycycline-treated mice harboring the KCa3.1+-transgene under the control of the reverse tetracycline-sensitive transactivator (rtTA) showed 800-fold channel overexpression above basal levels in the skin and solid KCa3.1-currents in keratinocytes. This overexpression resulted in epidermal spongiosis, progressive epidermal hyperplasia and hyperkeratosis, itch and ulcers. The condition was accompanied by production of the pro-proliferative and pro-inflammatory cytokines, IL-β1 (60-fold), IL-6 (33-fold), and TNFα (26-fold) in the skin. Treatment of mice with the KCa3.1-selective blocker, Senicapoc, significantly suppressed spongiosis and hyperplasia, as well as induction of IL-β1 (-88%) and IL-6 (-90%). In conclusion, KCa3.1-induction in the epidermis caused expression of pro-proliferative cytokines leading to spongiosis, hyperplasia and hyperkeratosis. This skin condition resembles

scholarship (C072/2014). BMB was supported by the NCATS (UL1 TR001860 and linked award TL1 TR001861). KLH received sabbatical support from the University of Otago. The funders had no role in study design, data collection and analysis, decision to publish, or preparation of the manuscript.

Competing interests: The authors have declared that no competing interests exist.

Abbreviations: CASP3, Caspase-3; DOX, Doxycycline; KCa3.1, intermediate-conductance calcium-activated potassium channel; PCNA, proliferating cell nuclear antigen.

pathological features of eczematous dermatitis and identifies KCa3.1 as a regulator of epidermal homeostasis and spongiosis, and as a potential therapeutic target.

Introduction

Ion channels have long been known to contribute to the pathophysiology of inflammatory, autoimmune [1], and proliferative diseases [2–4]. More recently, several calcium-permeable channels of the transient receptor potential family (TRP) and potassium channels have been found to be involved in skin conditions, such as melanoma [5], psoriasis [6], atopic dermatitis [7], Olmsted syndrome [8], and rosacea [9–11], suggesting the respective channels as potential treatment targets.

Although it has never been experimentally demonstrated to be present in the epidermis, one of the K^+ channels proposed to be a skin ion channels is the intermediate-conductance Ca^{2+}–activated K^+ channel, KCa3.1, encoded by the KCNN4-gene [12–14]. Its calmodulin mediated activation produces K^+ efflux and membrane hyperpolarization, thus serving well-known biological functions in other tissues, such as erythrocyte volume decrease [15,16], hyperpolarization-driven Ca^{2+}-influx, proliferation and cytokine production in T-cells [1, 17], migration and activation of macrophages/microglia [18,19], $Cl^-$and H_2O secretion in epithelia [20,21], as well as endothelium-derived hyperpolarization-mediated vasodilation [22,23].

From the pathophysiological perspective, KCa3.1 induction has been implicated in several diseases states characterized by excessive cell proliferation and inflammation (For recent in-depth reviews of KCa3.1 in health and as drug target in disease see [1,2, 24]. For instance, induction of KCa3.1 was shown to regulate the phenotypic switch of fibroblasts and smooth muscle cells towards a dedifferentiated proliferative phenotype that promoted pathological organ remodeling in the lung, heart, and kidneys [25–30], as well as arterial neointima formation [18, 31,32]. In addition, high expression of KCa3.1 has been considered a marker of tumor progression for some cancers [3, 33,34].

KCa3.1, therefore, can be viewed as a possible driver of disease, and several small molecule inhibitors for this therapeutically attractive target have been developed and tested in pre-clinical animal models [35,36]. The inhibitor, ICA-17043 (Senicapoc), initially intended for the treatment of sickle cell anemia, has been found clinically safe [37] and is currently being considered for drug repurposing for stroke and Alzheimer's disease, two conditions in which KCa3.1 contributes to the pathophysiology [19, 38].

However, concerning the skin, the physiological role of KCa3.1 and its pathophysiological significance for human skin disease is largely unexplored. So far, KCa3.1 protein expression and/or mRNA message have been found in rat epidermis [39], in human keratinocytes and melonama [5], where pharmacological inhibition of KCa3.1 has anti-proliferative efficacy in vitro. Yet, the role of KCa3.1 in the healthy or diseased epidermis remains elusive. Here, we hypothesized that epidermal KCa3.1, as a channel that controls cell volume, proliferation and chloride and water-secretion, is a regulator of epidermal homeostasis.

To test the hypothesis, we generated conditional KCa3.1-overexpressor mice (KCa3.1+) that harbor a murine *Kcnn4*-transgene under the control of a tetracycline response element (TRE) together with a rtTA-transgene [40] for DOX-inducible *Kcnn4*-transgene expression specifically in epithelia including the epidermis (Fig 1A) and found that KCa3.1-induction causes eczematous dermatitis characterized by intra-epidermal edema (spongiosis), epidermal hyperplasia and hyperkeratosis, severe itch, and ulcers.

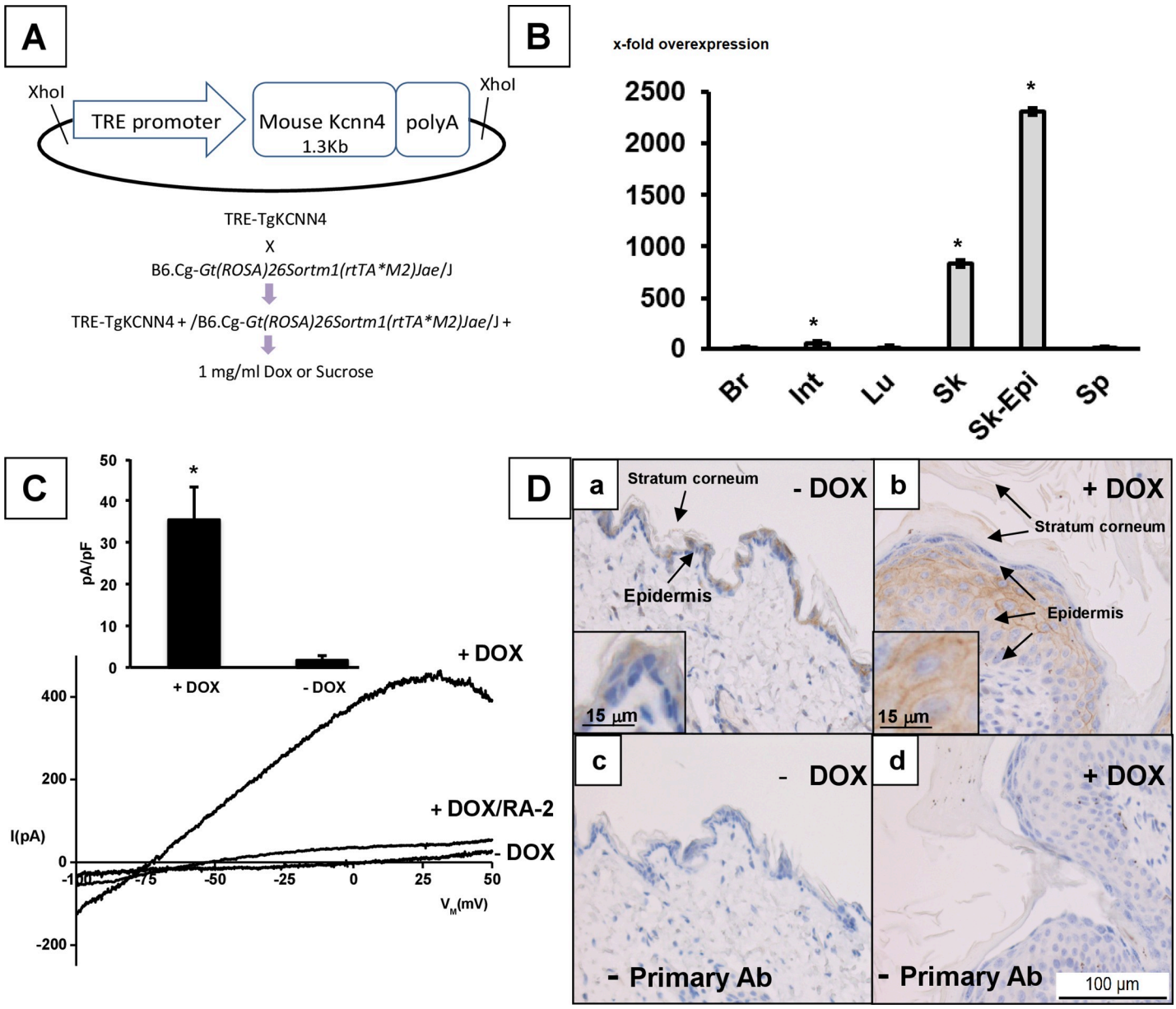

Fig 1. A) Plasmid construct for generation of *Kcnn4* transgenic mice and induction (gene product: KCa3.1) in epithelial tissues. B) Induction of KCa3.1 transgene expression by 2-weeks DOX-treatment over basal levels in various tissues as measured by qRT-PCR. Data (% of control (-DOX)) are given as means +/- SEM; *P<0.01, Student T test; Br, brain (DOX, n = 4; -DOX, n = 2); Int, small intestine (DOX, n = 7; -DOX, n = 6); Lu, lung (DOX, n = 11; -DOX, n = 10); Sk, skin (DOX, n = 7; -DOX, n = 6); Skin-Epi, skin epidermis (DOX, n = 7; -DOX, n = 2); Sp, spleen (DOX, n = 4; -DOX, n = 2). C) Whole-cell patch-clamp on freshly isolated keratinocytes from tail skin. Representative recordings of large KCa3.1 currents in keratinocytes (+DOX) from DOX-treated mice and currents in keratinocytes from untreated Ctrls (-DOX). Note: For an additional recording of small KCa3.1 currents in a keratinocyte from untreated Ctrl see S1A Fig. Inhibition of KCa3.1 currents by RA-2 at 1 μM. Inset: Summary data of KCa3.1-outward currents at a clamp potential of 0 mV. Data (pA/pF) are given as means +/- SEM (-DOX, n = 4; DOX n = 5); *P<0.01, Student's T test. D). Immune histochemical detection of KCa3.1 protein in the epidermis of DOX-treated mice (+DOX, n = 2) and an untreated mouse (-DOX): panels *a* and *b* with primary AB against KCa3.1; c and d without primary AB against KCa3.1. Inserts: 3 x zoom into epidermal layer.

https://doi.org/10.1371/journal.pone.0222619.g001

Material & methods

Transgenic mice

Our TRE-Tg*Kcnn4* mice were generated at Unitech Co., Ltd. (Chiba, Japan). Briefly, a tetracycline-regulated *Kcnn4* expression construct was generated by subcloning PCR-amplified

Table 1. Primers for PCR and qRT-PCR.

Gene	Forward	Reverse	Accesion No.
EREG	TGGGTCTTGACGCTGCTTTGTCTA	AAGCAGTAGCCGTCCATGTCAGAA	NM_007950.2
GAPDH	AGGGAGATGCTCAGTGTTGG	CAATGAATACGGCTACAGCAAC	NM_001289726.1
HB-EGF	CAGGACTTGGAAGGGACAGA	CCCTAACCCCTTTCCTTTCTT	NM_010415.2
HGF	CATTGGTAAAGGAGGCAGCTATAAA	GGATTTCGACAGTAGTTTTCCTGTAGG	NM_001289460.2
IL-1β	TGCCACCTTTTGACAGTGATG	AAGGTCCACGGGAAAGACAC	NM_008361.4
IL-6	TCTGCAAGAGACTTCCATCCA	AGTCTCCTCTCCGGACTTGT	NM_031168.2
TGFα	CTGTGTGCTGATCCACTGCT	CAAGCAGTCCTTCCCTTCAG	NM_031199.4
TNFα	CCCACGTCGTAGCAAACCAC	GCAGCCTTGTCCCTTGAAGA	NM_013693.3
KCa3.1	GTCTGCTGCACAGCTCTCCT	TCCTTCCTTCGAGTGTGCTT	NM_008433.4

https://doi.org/10.1371/journal.pone.0222619.t001

cDNA encoding the open reading frame of murine *Kcnn4* (gene ID16534)) into the pTRE--Tight expression vector (Clontech). The construct was verified by sequencing. The pTRE--Tight vector construct was cleaved with the restriction enzyme and injected into pronuclei of fertilized mouse oocytes of the C57BL/6J strain. The putative TRE-Tg*Kcnn4* founders obtained were genotyped by PCR with primers specific for the murine *Kcnn4* sequence. Two founders were crossed with wild type C57BL/6J mice to establish the F1 generation. One line was inbred over 2–3 generations and then crossed with B6.Cg-Gt(ROSA)26Sortm1(rtTA*M2)Jae/J + [40]. Routine genotyping was performed by using DNA from tail tips and PCR primers (see Table 1) and the SuperHotTaq Master mix (BIORON GMBH, Germany); cycle program: 94˚C for 2 min, 35 cycles 94˚C for 20 sec, 56˚C for 30 sec, 72˚C for 30 sec, and cooling to 10˚C. PCR products were separated by gel electrophoresis (1.5% agarose). Pups of both sex being hemizygous for both transgenes were used for later experimentation (age range 8–20 weeks). All transgenic mice were generated and maintained within a specific pathogen free (SPF) barrier facility of Aragonese Center for Biomedical Research according to local and national regulations.

For transgene-induction over 1 or 2 weeks, doxycycline (DOX, Sigma) was added to the drinking water (1mg/ml) and water intake was monitored. Senicapoc was synthesized in-house as previously described [41]. Senicapoc-medicated chow was prepared to administer a dose of 30 mg/kg/day during the entire DOX-treatment until sacrifice. We did not include a group of control mice (-DOX) treated with senicapoc since even higher doses of senicapoc had previously been found to be safe in mice when administered for 3 months [41]. The Photo- and video-documentation was routinely performed at the day of or the day prior to sacrifice. Organs and blood were collected after CO_2 suffocation and stored on dry ice or fixed in neutral-buffered formaldehyde (4%) until further processing. All procedures were approved by the Ethics Committee for Animal Research of the University of Zaragoza (PI27/13; PI28/12; PI37/13/16; PI32/15) and in accordance with the ARRIVE guidelines.

Isolation of epidermis and epidermal keratinocyte

Tails were sterilized by short immersion in 90% ethanol and then stored in MEM-Earle with 20 mM HEPES until further processing. For separation of the skin from the underlying tissue, the skin was carefully cut open and removed from the base to the tip of the tail and cut into approximately 0.5 cm^2 large pieces. Thereafter, pieces floated on a 0.25% trypsin/phosphate-buffered solution (PBS) overnight. For keratinocyte isolation, epidermis was carefully separated from the rest of skin (consisting mainly of remaining epidermal hair follicles, dermis, fatty and connective tissue) and was cut into small pieces using a scalpel. Keratinocytes were

dispersed by repeated passing through the tip of a cell culture pipette, seeded on coverslips in MEM Earle supplemented with 10% calf serum, and used for patch-clamp experiments within the next 3 hrs.

Patch-clamp electrophysiology

Ca^{2+}-activated K^+ currents in murine keratinocytes were measured in the whole-cell configuration using an EPC10-USB amplifier (HEKA, Electronics, Lambrecht-Pfalz, Germany) and a pipette solution (intracellular) containing 1 μM Ca^{2+} free for channel activation (in mM): 140 KCl, 1 $MgCl_2$, 2 EGTA, 1.71 $CaCl_2$ (1 μM $[Ca^{2+}]_{free}$) and 5 HEPES (adjusted to pH 7.2 with KOH). The free Ca^{2+} concentration was calculated with the MaxChelator program (https://somapp.ucdmc.ucdavis.edu/pharmacology/bers/maxchelator/webmaxc/webmaxcS.htm). The bath solution contained (in mM): 140 NaCl, 5 KCl, 1 $MgSO_4$, 1 $CaCl_2$, 10 glucose and 10 HEPES (adjusted to pH 7.4 with NaOH). For KCa3.1 inhibition, we applied 1,3-Phenylenebis (methylene)bis(3-fluoro-4-hydroxybenzoate (RA-2) at a concentration of 1 μM (n = 2, experiments). Data acquisition and analysis was done with the Patch-Master program (HEKA). Ohmic leak conductance of up to 1 nS was subtracted where appropriate. We quantified outward currents at a potential of 0 mV. Membrane capacitance was 6 +/- 1 pF (n = 4) in keratinocytes from Dox-treated mice and 7 +/- 2 pF (n = 5) in keratinocytes from non-treated mice.

Histology

Samples were fixed in 4% formaldehyde for at least 24 hrs and then transferred to 60% ethanol. Thereafter samples were imbedded in paraffin and cut into 4 μm-thick sections. Sections were stained with hematoxylin and eosin. Scoring: For quantifying and comparing the skin pathology, skin sections were scored for grade of hyperplasia, and hyperkeratosis by a pathologist (MM) and for grade of intra-epidermal edema by two investigators (RK/KLH), independently and in a blinded fashion. We used the following in-house developed scoring system: Mild: $\geq 0.5 < 1$; Moderate: $\geq 1 < 2$; Severe: ≥ 2. Individual scores for intra-epidermal edema did not vary by more than 0.5 and were averaged.

Immunohistochemistry and TUNEL assay

For KCa3.1, tissue samples were fixed in 4% neutral buffered formaldehyde solution and embedded in paraffin. 2.5 μm-thick sections were cut with a rotation microtome (Leica RM2255). Slides were air dried at 37˚C overnight, were de-paraffinized in xylene for 10 min, and then rehydrated. After rehydration, epitope retrieval was carried out using the PT Link (Dako) at 95˚C for 20 min in a high pH buffer (Dako Antigen retrieval, high pH). Endogenous peroxidase was blocked using the EnVision FLEX Peroxidase-Blocking kit followed by two washes for 5 min each (Dako wash buffer). Sections were incubated for 60 min with a rabbit anti-KCNN4 primary antibody (AV35098, Sigma-Aldrich) at 1/2000 dilution followed by two washes. Signal amplification was done using the ImmPRESS™ Excel Amplified HRP Polymer Staining Kit (Vector Laboratories). After 3 wash steps (Dako wash buffer, 5 min each). Sections were incubated with 3,3'-diaminobenzidine (DAB) for 10 min and counterstained with hematoxylin.

Proliferating cell nuclear antigen (PCNA) and Caspase 3 (CASP3): 5 μm-thick tissue sections were placed on silanated slides. After de-paraffinization, endogenous peroxidase was quenched by immersing the samples in methanol containing 0.03% hydrogen peroxide. Heat antigen retrieval was performed in pH 6.5 10 μM citrate-based buffered solution (Dako). In order to prevent non-specific binding, samples were incubated for 2 h with Protein Block (Dako). Samples were incubated overnight at 4˚C with mouse and rabbit monoclonal

antibodies against PCNA (Cell Signaling, 1:100) and Cleaved-CASP3 (Calbiochem, 1:100), respectively, followed by incubation with an anti-mouse or anti-rabbit polymer-based Ig coupled with peroxidase (Cell Signaling) for 30 min at RT. Then, sections were incubated with 3,3'-diaminobenzidine (DAB) and counterstained with hematoxylin, and studied under an Olympus BX-61 microscope.

Apoptosis was determined by using the TUNEL (Terminal deoxynucleotide transferase mediated X-dUTP nick end labeling) assay. 5 μm-thick sections were de-paraffinized and rehydrated. Then, sections were treated with Proteinase K (20 μg ml–1, 15 min, at RT) and rinsed twice with phosphate buffered saline (PBS). For detection of apoptotic nuclei, sections were incubated for 1 hrs at 37˚C in the dark with the *in situ* Cell Death Detection Kit (Roche) according to the manufacturer's instructions. After two washes with PBS, sections were mounted in ProLong® with DAPI (Life technologies). Fluorescence-microscopy was performed with an Olympus BX-61 epi-fluorescence microscope equipped with filter sets for fluorescence microscopy: ultraviolet (UV, 365 nm, exciting filter UG-1) and blue (450–490 nm, exciting filter BP 490). Photographs were taken with a digital Olympus CCD DP70 camera.

RNA isolation, reverse transcription, and quantitative RT-PCR

Depilated skin of the neck and other organs were placed into 1 ml TriReagent (Sigma, Saint Louis, Missouri, USA) and stored at -80˚C. Samples were homogenized with a T10 basic ULTRA-TURRAX (IKA, Staufen, Germany) at 4˚C.

Total RNA was isolated with the TriReagent following the manufacturer's protocol, and further purified using RNA Clean-up and Concentration-Micro-Elute kit (Norgen Biotek, Thorold, Canada). Genomic DNA was digested using the Ambion DNA-free kit (Invitrogen, Carlsbad, California, USA). Quantity and purity of extracted RNA were determined by spectrophotometry (NanoDrop1000, Thermofisher, Waltham, MA) and stored at −80˚C for later use. Integrity of RNA samples and successful digestion of genomic DNA were verified by gel electrophoresis. Reverse transcription was performed with 600 ng of total RNA by using the Super Script III reverse transcriptase (Invitrogen, Carlsbad, California, USA) and random hexamers following the manufacturer's protocol.

cDNA obtained from 10 ng of total RNA was amplified in triplicates using the SYBR Select Master Mix and a StepOnePlus Real-Time PCR system (Applied Biosystems, Foster City, California, USA) using the following cycle protocol: 95˚C, 15 s and 60˚C, 60 s repeated for 40 cycles. As final step, a melting curve analysis was carried out to verify correct amplification. The primers are given in Table 1. Data were analyzed with LinReg PCR software and gene expression levels relative to *Gapdh* expression as reference gene and normalized to control were calculated using the formula: $\%\ of\ Gapdh = Efficiency^{Cq(Gapdh)-Cq(GOI)} x100$. The values were used to calculate ratio values (DOX/-DOX; Senicapoc/Ctrl) given in graphs.

LC-MS analysis

A 10 mM stock solution of Senicapoc (from in-house organic synthesis) was prepared by dissolving 6.4 mg Senicapoc in 2 ml acetonitrile. Working standard solutions were obtained by diluting the stock solution with acetonitrile.

Preparation of plasma samples: Commercial SPE cartridges (Hypersep C18, 100 mg, 1 ml) were purchased from Thermo Scientific (Houston, TX, U.S.A). Before extraction, cartridges were conditioned with acetonitrile, 2 × 1 ml, followed by water, 2-times × 1 ml. After loading the SPE cartridges with plasma samples, they were washed successively with 1 ml each of 20% and 40% acetonitrile in water followed by elution with 2 ml of acetonitrile. Elute fractions were collected and evaporated to dryness, under a constant flow of air, using a PIERCE Reacti-

Vap^{TM} III evaporator (PIERCE, Il, USA). The residues were reconstituted using 200 μl acetonitrile and were used for LC-MS analysis.

Preparation of skin samples: A 100 mg of depilated skin sample was homogenized thoroughly in 2.0 ml of acetonitrile in a gentleMACS™ M tube using a gentleMACS™ Dissociator (Miltenyi Biotec Inc., CA, USA). Each sample was subjected to three cycles of the preprogrammed homogenization protocol Protein_01.01 (a 55 s homogenization cycle with varying speeds and directions of rotation). Homogenized samples were centrifuged for 10 min at 4000 rpm. Each supernatant was collected in a 4 ml glass vial and was evaporated to dryness, under a constant flow of air, as described above. The residues were reconstituted in 100 μl acetonitrile and were used for LC-MS analysis.

LC/MS analysis was performed with a Waters Acquity UPLC (Waters, NY, USA) equipped with a Acquity UPLC BEH 1.7 μM C-18 column (Waters, New York, NY) interfaced to a TSQ Quantum Access Max mass spectrometer (MS) (Thermo Fisher Scientific, Waltham, MA, USA). The isocratic mobile phase consisted of 80% acetonitrile and 20% water, both containing 0.1% formic acid with a flow rate of 0.25 ml per minute. Under these conditions, Senicapoc had a retention time of 0.80 minute.

Using Heated electrospray ionization source (HESI II) in positive ion mode, capillary temperature 250˚C, vaporizer temperature: 30˚C, spray voltage 3500 V, sheath gas pressure (N_2) 60 units, Senicapoc was analyzed by the selective reaction monitoring (SRM) transition of its molecular ion peak 324.09 (M+1) into 228.07, 200.07,183.11 and 122.18 *m/z*. An 8-point calibration curve from 50 nM to 10 μM concentration range was used for quantification.

Statistics

Data in text and graphs are means +/- standard error of the mean (SEM), if not stated otherwise. If not otherwise stated, we used the unpaired Student's T Test (two-tailed) for comparison of data sets. The significance level was set to a P value of <0.05.

Results

KCa3.1 induction in skin

Doxycycline(DOX)-treatment with 1 mg/ml in drinking water produced a 833-fold KCa3.1-overexpression in the skin, 2310-fold KCa3.1-overexpression, particularly, in the epidermal layer, and a 46-fold overexpressing in the intestine (Fig 1B). In bone marrow, brain, lung, skeletal muscle, spleen, KCa3.1-mRNA levels were similar to untreated mice.

Patch-clamp electrophysiology studies in isolated keratinocytes revealed a strong induction of KCa3.1-function in DOX-treated KCa3.1+ mice. The KCa3.1-currents demonstrated the typical fingerprint characteristics of KCa3.1, which were activation by 1 μM Ca^{2+}, voltage-independent, and mildly inwardly-rectifying. RA-2 (1 μM), a negative-gating modulator of KCa2/3 channels [42], blocked the KCa3.1 current. KCa3.1-induction was not found in untreated mice and KCa3.1 outward-currents were small or difficult to discriminate from background currents in most cells (Fig 1C). In fact, we saw a clearly distinguishable KCa3.1 current in only 1 of 5 cells (S1A Fig).

We examined the KCa3.1-protein expression by immune histology (Fig 1D) and identified immune reactivity in the thin epidermal layer of untreated mice and appreciable immune reactivity in the thicker epidermal layer of DOX-treated mice (see following paragraphs).

Together, these findings demonstrate strong induction of KCa3.1-transgene expression and function in the skin and, particularly, in the epidermis.

Skin phenotype and behavioral alterations in DOX-treated KCa3.1+ mice

The DOX-treated KCa3.1+ mice of both sexes appeared normal during the 1st week of the treatment and then developed progressive skin pathology with generalized piloerection, intense scratching behavior (S Movie 1), scaly skin patches, and in some mice overt ulcerative lesions, mainly visible in the neck areas, chest, and ears (Fig 2).

Histology (Fig 3A to 3D) of neck skin showed moderate to severe hyperplasia of the epidermis, affecting also the hair follicles within the dermis, and substantial hyperkeratosis. In the epidermis of the DOX-treated mice, we found foci of moderate intra-epidermal edema (Fig 3D), similar to spongiosis, which is characteristic of eczematous dermatitis [43]. The phenotype was completely reversible within 6 weeks when DOX was removed after 9 days of treatment (see S1B Fig).

At an earlier time point (1-week DOX), we recorded the same degree of intra-epidermal edema and an early stage of hyperplasia and hyperkeratosis (Fig 3C and S1C Fig). Yet, at first sight, the mice appeared healthy. Concerning controls, a 2-week DOX-treatment of the inducer strain (R26-rtTA-M2) or of *Kcnn4*-transgene-harbouring mice lacking the rtTA induced no observable skin pathology (S1D Fig).

Immune histology on KCa3.1+ skins of the neck region showed high-expression of the proliferating cell nuclear antigen (PCNA), a marker of cell proliferation, in the hyperplastic epidermal layer of 2-week DOX-treated mice (Fig 3E and S1E Fig). In the untreated control

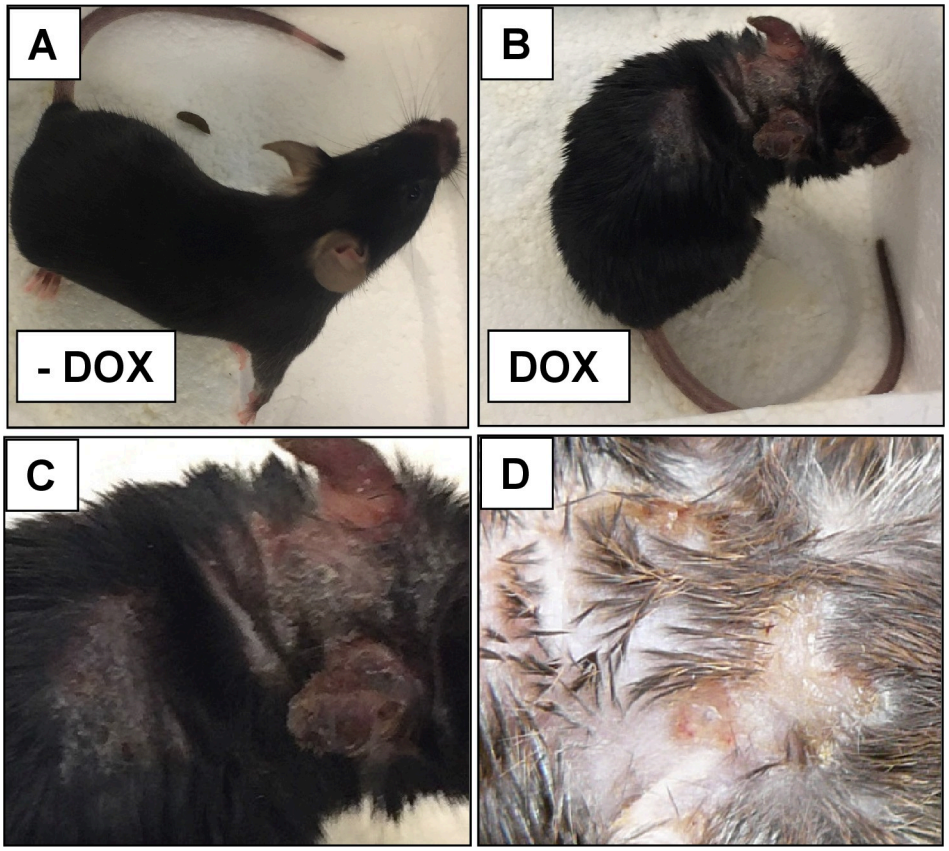

Fig 2. Macroscopic skin pathology DOX-treated KCa3.1+ mice. Photographs of A) untreated Ctrl (-DOX), B) DOX-treated KCa3.1+, C) higher magnification of the neck shown in B, D) patchy erythematous and scaly skin with ulcerative areas of a DOX-treated mouse. Note: Videos of DOX-treated mice showing severe scratching behavior and of Ctrls are found in the supplement.

https://doi.org/10.1371/journal.pone.0222619.g002

animals, uniform immune reactivity was observed in the nuclei of keratinocytes lining the basal epidermal layer. We also stained for CASP3, another marker of apoptosis, and did not find induction of CASP3 in the hyperplastic epidermal layer or in the dermis, with the exception of ulcerative sites (S1E Fig). No CASP3 immune reactivity was seen in keratinocytes of the epidermis of untreated controls (S1F Fig). Apoptosis as measured by TUNEL was not found at hyperplastic sites (Fig 3F), but at wound areas with substantial tissue destruction (S1E Fig).

Together, these data demonstrate that induction of KCa3.1 produces moderate intra-dermal edema (sub-acute spongiosis) and drives keratinocyte proliferation, but does not cause generalized cell toxicity and cell death. The localized epidermal damage and ulcers are likely the result of the intense scratching behavior.

Alterations of cytokine expression profile in skin

To shed light on the mechanisms, by which KCa3.1-induction in the keratinocytes produced spongiosis and epidermal hyperplasia, we measured the mRNA-expression of several pro-proliferative cytokines that are known to promote keratinocyte proliferation in an auto-stimulatory or autacoid fashion [44] (Fig 4). It is worth mentioning that KCa3.1-KO and/or inhibition have been shown to reduce IL-β1 and TNFα levels in activated microglia after cerebral infarction [19].

In the skin, we found strongly increased mRNA expression of IL-β1 (60-fold), IL-6 (33-fold), and TNFα (26-fold). Expression levels of HGF and TGFα and a series of other growth factors were not significantly altered (for more details see Fig 4A).

The induction of IL-β1 and TNFα expression was higher in the epidermal layer than in the underlying skin tissue and the data thus demonstrate strong cytokine induction in keratinocytes (Fig 4B).

Systemic KCa3.1 channel blockade reduces skin pathology

We next tested whether pharmacological blockade of KCa3.1 functions can suppress this phenotype and treated the mice with Senicapoc-containing chow at a dose of 30mg/kg/day [45] during the 2-weeks of DOX treatment.

The Senicapoc treatment gave rise to total plasma concentrations of 254+/-61 nM (n = 11) and tissue levels in the skin of 2.9+/-0.9 μM (n = 4) at the time of sacrifice. At these total concentrations (and assuming a protein binding of 90%), pharmacological inhibition of the channel can be expected because concentrations of Senicapoc in the skin are at least 2 orders of magnitude above the reported IC_{50} of 10 nM [12, 37].

As shown in Fig 5A, we report that the Senicapoc treatment did not prevent the pathological skin alterations, but significantly reduced intra-epidermal edema by ≈60%, hyperplasia by ≈50%, as well as a trend in reduction of hyperkeratosis and fibrosis.

Overall, this Senicapoc trial suggests that the skin pathology was caused largely by the induced function of KCa3.1 and demonstrates that Senicapoc is able to reduce the earliest strong alteration, i.e. intra-epidermal edema (Fig 3C and 3D), presumably by blocking KCa.3.1-induced disturbances of epidermal water-salt homeostasis.

Considering cytokine levels in the skin (Fig 5B), Senicapoc significantly reduced mRNA-expression levels of IL-β1 (≈-88%) and of IL-6 (≈-90%) when compared to DOX-treated control animals, while TNFα mRNA-expression levels were unchanged. These lower levels of pro-proliferative cytokines could explain the lower degree of hyperplasia.

Discussion

The present study introduces a genetic model of epidermal KCa3.1-induction to investigate the physiological and potential pathophysiological significance of this channel capable of

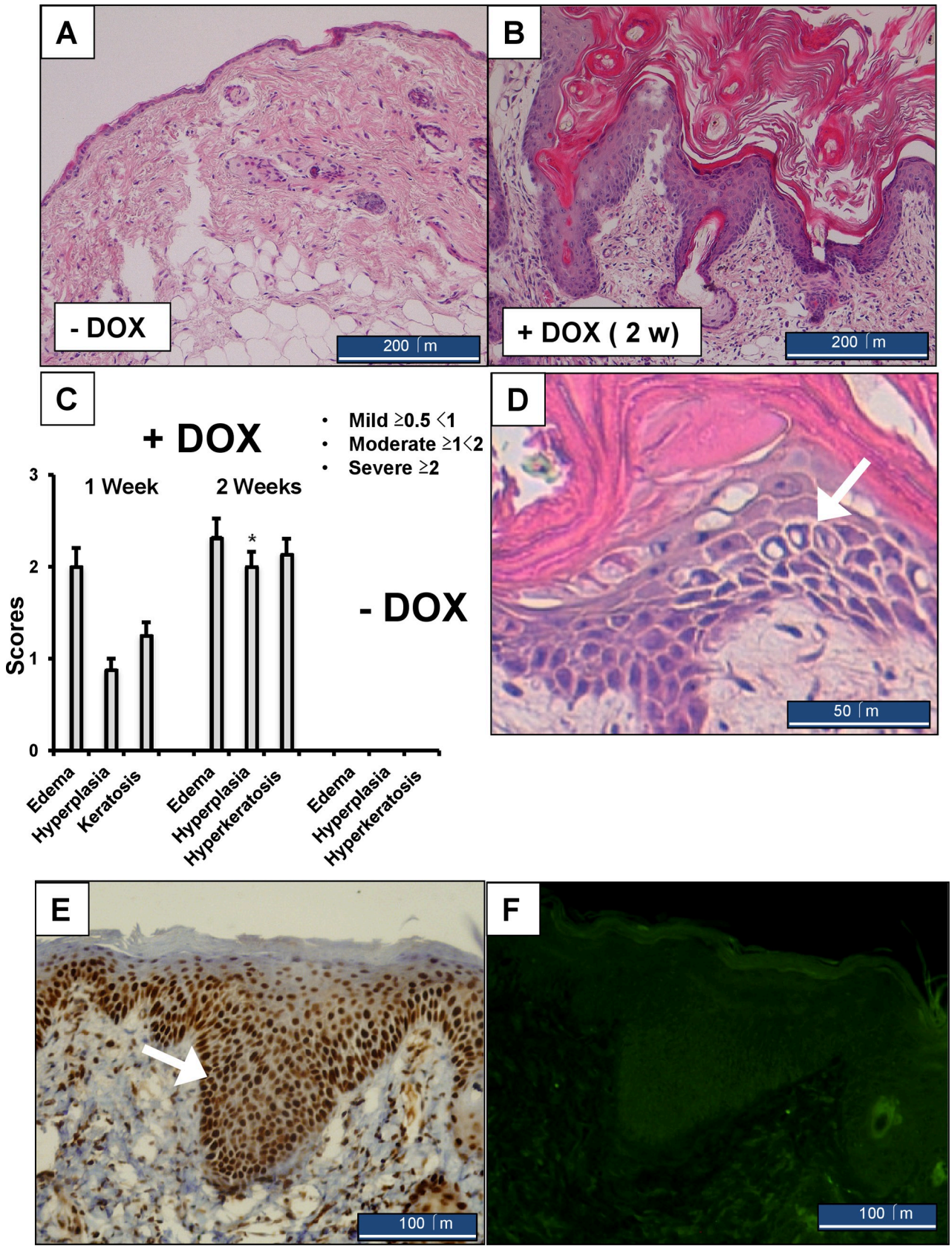
A
- DOX
200 m
B
+ DOX (2 w)
200 m
C
+ DOX
• Mild ≥0.5 <1
• Moderate ≥1<2
• Severe ≥2
1 Week
2 Weeks
Scores
3
2
1
0
*
- DOX
Edema
Hyperplasia
Keratosis
Edema
Hyperplasia
Hyperkeratosis
Edema
Hyperplasia
Hyperkeratosis
D
50 m
E
100 m
F
100 m

Fig 3. Histological evaluation of skin pathology in KCa3.1+ mice. H&E-stained sections of normal skin of the neck region from an untreated mouse (A) and a skin of the same region from a DOX-treated KCa3.1+ (B) with severe hyperplasia and hyperkeratosis. C) Summary of pathology scores. Data are given as means +/- SEM, n = 4 (1 week DOX), n = 26 (2 weeks DOX), n = 15 (Ctrls); *P < 0.05 vs. 1 week DOX, Student's T test. Note that the scores for Ctrl skin are 0. D) Higher magnification of the hyperplastic epidermis of DOX-treated KCa3.1+. Note the presence of intra-epidermal edema with enlarged intra-cellular space (indicated by white arrow). E) Immune histological stains of the proliferation marker, PCNA, in the hyperplastic epidermis of DOX-treated KCa3.1+. Note the intense staining of the basal layer (white arrow) that becomes weaker when approaching the stratum corneum (representative image from 3 mice). F). The TUNEL assay detected no apoptotic keratinocytes in the hyperplastic epidermis.

https://doi.org/10.1371/journal.pone.0222619.g003

controlling cell volume, growth, and cellular salt/water homeostasis in the epidermis. In fact, it is the first study describing the consequences of genetically encoded induction of an ion channel above basal levels in the skin. Our results demonstrate that KCa3.1 over-expression was capable of causing a severe disturbance of epidermal homeostasis.

This is based on the following lines of evidence: 1) KCa3.1-induction produced intra-epidermal edema (spongiosis). 2) KCa3.1-induction produced progressive epidermal hyperplasia and hyperkeratosis causing severe itch and ulcers. Finally, 3) KCa3.1-induction strongly up-regulated epidermal (i.e., keratinocyte) synthesis of the pro-proliferative, auto-stimulatory,

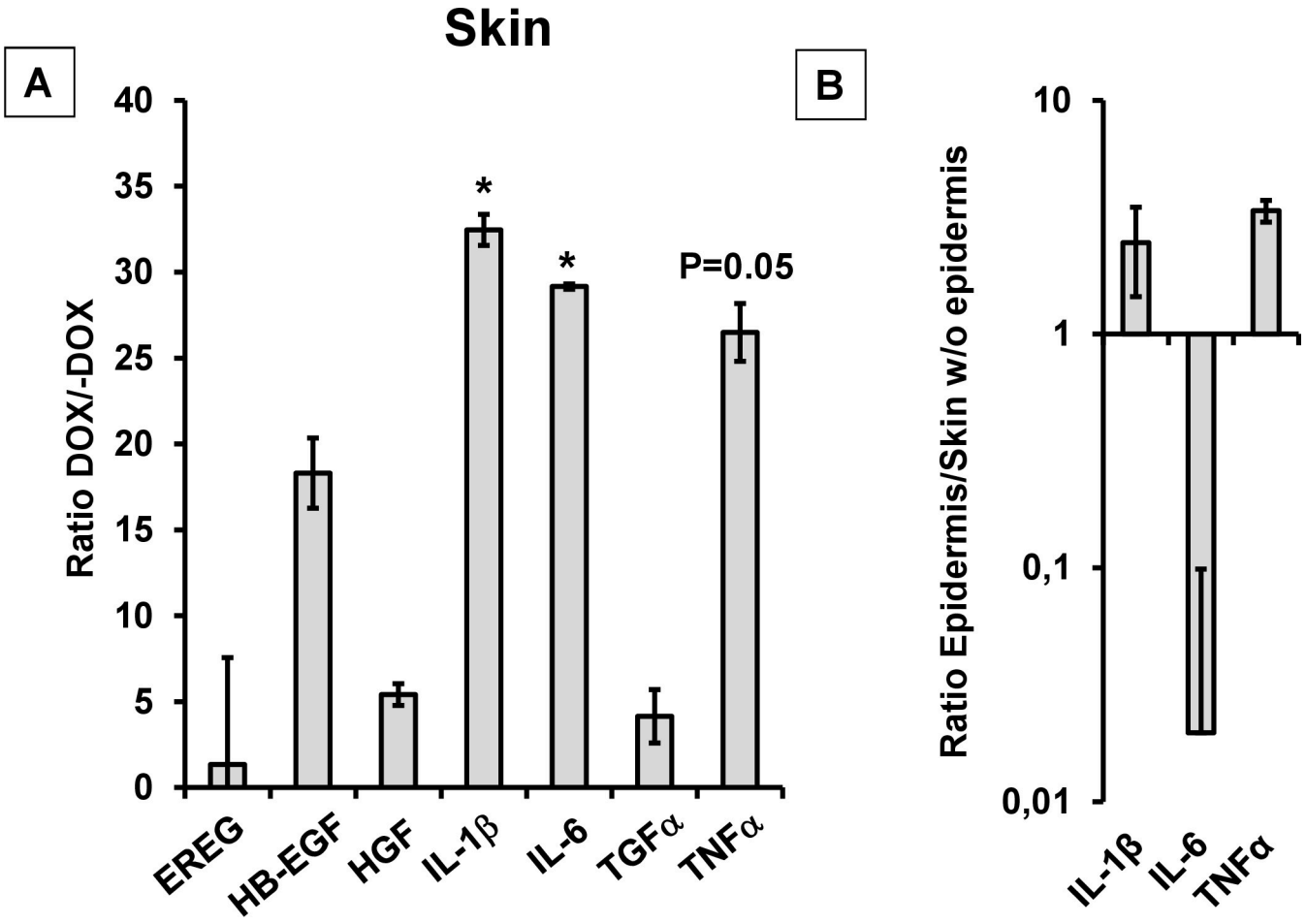

Fig 4. Cytokine mRNA-expression profile. (A) Alterations of cytokine mRNA-expression profile in DOX-treated KCa3.1+ mice (DOX/-DOX). (B) Cytokines with higher expression in the epidermis than in the underlying skin tissue (epidermis/ skin w/o epidermis). EREG, epiregulin (dox, n = 5; -DOX, n = 5); HB-EGF, Heparin-binding EGF-like growth factor (DOX, n = 5; -DOX, n = 5); HGF, Hepatocyte growth factor (DOX, n = 5; -DOX, n = 5), Interleukin (IL)-1β (DOX, n = 7; -DOX, n = 7), IL-6 (DOX, n = 7; -DOX, n = 7), TGFα, transforming growth factor α (DOX, n = 5; -DOX, n = 5); TNFα; tumor necrosis factor-α (DOX, n = 5; -DOX, n = 5). Data (DOX/-DOX; Epidermis (n = 4/Skin w/o Epidermis (n = 4)) are given as means +/- SEM; *P<0.05, Student's T test.

https://doi.org/10.1371/journal.pone.0222619.g004

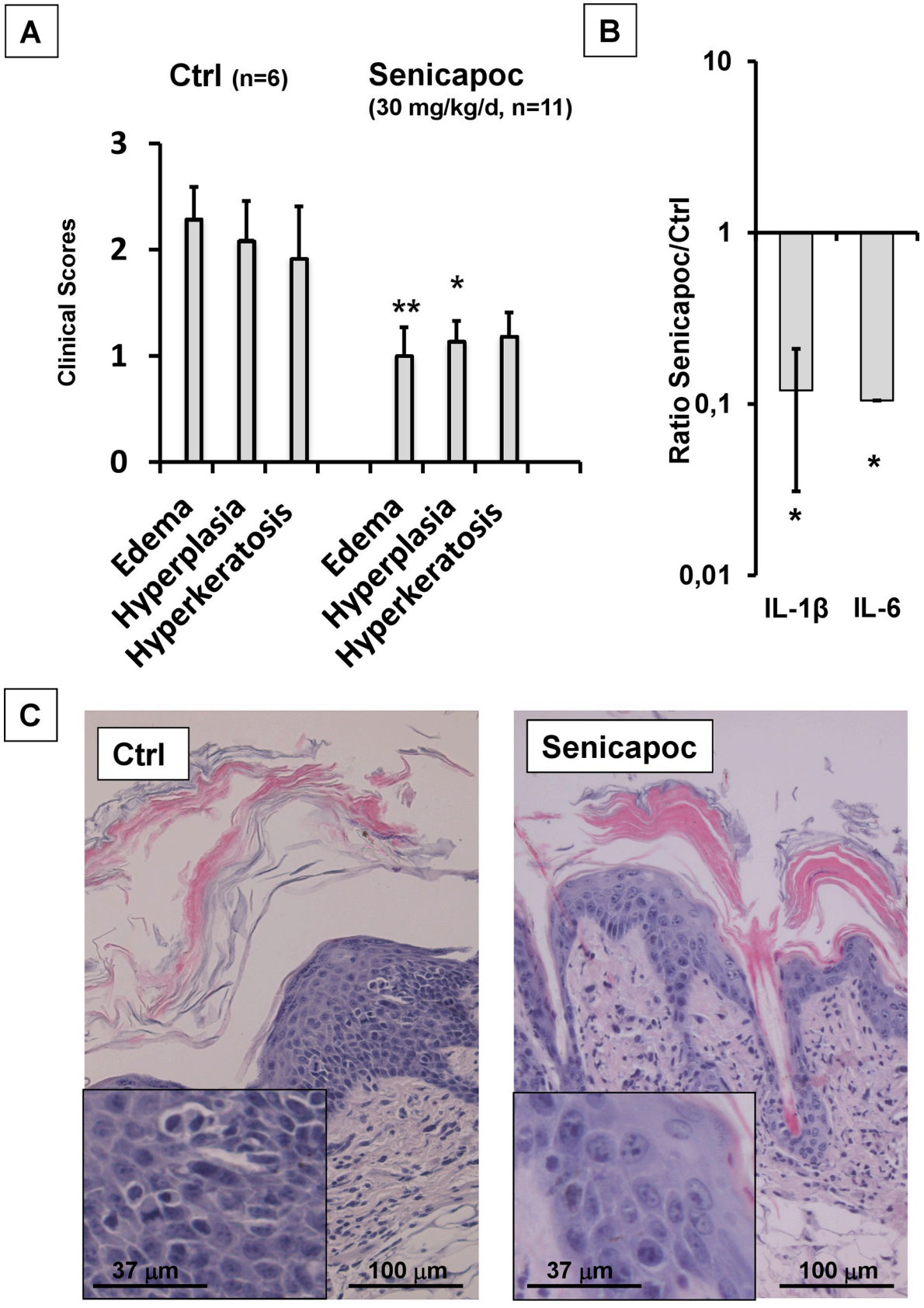
A
Ctrl (n=6)
Senicapoc
(30 mg/kg/d, n=11)
Clinical Scores
3
2
1
0
**
*
Edema
Hyperplasia
Hyperkeratosis
Edema
Hyperplasia
Hyperkeratosis
B
Ratio Senicapoc/Ctrl
10
1
0,1
0,01
*
*
IL-1β
IL-6
C
Ctrl
Senicapoc
37 μm
100 μm
37 μm
100 μm

Fig 5. Senicapoc suppressed skin pathology (A) and induction of IL-1β and IL-6 in DOX-treated KCa3.1+ mice (B). Data (Senicapoc/Ctrl) are given as means +/- SEM, n = 5 each, $^{*}P<0.05$, $^{**}P<0.01$ Student's T test. C) Examples of skin pathology in DOX-treated KCa3.1+ mice receiving vehicle or Senicapoc. Inserts: 2.7-digital zoom-into epidermis showing lower grade of intra-epidermal edema in Senicapoc-treated mice.

https://doi.org/10.1371/journal.pone.0222619.g005

and pro-inflammatory cytokines, in particular, IL-β1, IL-6 and—by trend—TNFα. Taken together, KCa3.1-induction in the epidermis produced skin pathology in mice that resembled the pathological features of itchy eczematous dermatitis [43].

The physiological and pathophysiological significance of KCa3.1 in the skin has been elusive until now. So far, keratinocyte KCa3.1 has been studied–superficially though—by mRNA-expression experiments in cultured human keratinocytes [5] and immune histochemistry in rat epidermis [39], which did not provide much information about the role of the channel in epidermal homeostasis *in-vivo*. Here, we intended to provide new knowledge by generating a murine model of genetic conditional induction of a murine KCa3.1-transgene in epidermis (Fig 1).

The KCa3.1 induction in DOX-treated animals was highly selective for skin epidermis as concluded from 833-fold overexpression. Concerning other tissues, we found a much less pronounced 46-fold overexpression in the intestine (see below).

We confirmed KCa3.1 transgene function after *in-vivo* DOX-treatment by patch-clamp electrophysiology on isolated keratinocyte, which unequivocally revealed large KCa3.1-currents being sensitive to a KCa3.1-inhibitor displaying the biophysical and pharmacological characteristics of KCa3.1 (Fig 1C) [12]. In keratinocytes from untreated mice, KCa3.1 currents were very small or undetectable suggesting low basal channel expression or a few KCa3.1-expressing cells. IHC demonstrated appreciable immune reactivity in the hyperplastic epidermis of the DOX-treated mice. Immune reactivity was also found in the thin epidermis of untreated mice, suggesting some constitutive protein expression in addition to mRNA-expression of KCa3.1 (Fig 1D).

A major outcome of our study was that KCa3.1-induction produced visibly piloerection, scaly skin patches, and intense scratching behavior that in turn gave rise to bloody ulcerative lesions (Fig 2 and S1 Movie). These symptoms are similar to those of itchy eczematous dermatitis in humans [43]. In analysis of histological sections, we observed intra-epidermal edema (sub-acute spongiosis) and ensuing progressive hyperplasia, and hyperkeratosis as histological features of chronic eczema [43].

It is also worth mentioning that sub-chronic conditional gene deletion of KCa3.1 in the epidermis as well as life-long KCa3.1-deficiency [16] complete did not produce any skin alterations, indicating that basal KCa3.1 expression is apparently not crucial for epidermal homeostasis. In keeping with the induction of KCa3.1 in the small intestine, we also demonstrate a mild intestinal phenotype characterized by moderate chyme accumulation and lower propulsive spontaneous motility, which is the content of a separate report [46].

Concerning the cellular mechanisms, by which KCa3.1-induction produced this skin condition, the morphological and molecular biological alterations described here agree well with the known physiological functions of KCa3.1 [12]: 1) The intra-epidermal edema can be explained by KCa3.1's ability to move K^+ and concomitantly water and Cl^- into the extracellular compartment [13, 15, 20]. Overexpression of the channel could do this in an excessive manner leading to the observed expansion of the extracellular compartment and/or cell shrinkage producing intracellular gaps. In fact, intra-epidermal edema was already pronounced at the early time point (1 week), when hyperplasia and hyperkeratosis was still in an initial phase. Intra-epidermal edema was of similar grade later, when hyperplasia and hyperkeratosis

progressed further. Therefore, intra-epidermal edema can be considered the starting point for the latter alterations.

2) In addition to its function as a K^+ secreting channel, KCa3.1 activity is known to produce strong membrane hyperpolarization, which in turn potentiates calcium-influx enabling long-lasting elevations in $[Ca^{2+}]_I$ (for review see: [1, 36]). In several cell systems, this elevation of $[Ca^{2+}]_I$ has been shown to be required for the sustained initiation of several cellular processes, including proliferation and migration [1, 47]. KCa3.1-mediated hyperpolarization and ensuing amplification of $[Ca^{2+}]_I$ signaling is known to regulate cytokine production in T cells, activated fibroblasts or smooth muscle cells (for review see: [1]). Accordingly, inhibition or genetic knockdown of the channel has been reported to reduce IL-2 production by T cells [47,48] and IL-β1 and TNFα levels by microglia in ischemic stroke [19]. Here, we showed that the reverse maneuver (induction) resulted in a higher expression of IL-β1 and–by trend- TNFα in keratinocytes of the epidermis (Fig 5). This keratinocyte cytokine production may drive hyperplasia and hyperkeratosis in an auto-stimulatory fashion.

Considering the impressive magnitude of hyperplasia and hyperkeratosis (Fig 3), we speculate that this is a secondary and overshooting repair mechanism in response to intra-epidermal edema and epidermal destabilization.

In summary, we provide first mechanistic evidence that KCa3.1 induction produced skin pathology *in-vivo* by causing extracellular fluid accumulation and epidermal destabilization as a primary event and secondary phenotypic switch to a proliferative keratinocyte phenotype (PCNA-high, Fig 3E), producing epidermal hyperplasia.

It is worth mentioning that the selective KCa3.1-blocker Senicapoc significantly prevented both the primary intra-epidermal edema and the subsequent hyperplasia (Fig 5). The prevention of edema is somewhat reminiscent of the reported reduction in *in-vitro* cyst formation by kidney cells from patients with autosomal-dominant polycystic kidney disease with a KCa3.1 blocker [25]. Moreover, Senicapoc treatment lessened increases of IL-β1 and IL-6 mRNA-expression levels in the affected skin (Fig 5). These data strongly suggest that these morphological alterations and the higher expression of pro-proliferative cytokines are mediated by KCa3.1 channel function, and likely act as mechanistic drivers of epidermal hyperplasia. Because the treatment did not fully suppress the phenotype, we cannot fully exclude additional local or systemic mechanisms.

There are some limitations applying to this study: While the qRT-PCR quantification of KCa3.1-transgene induction in the skin and the epidermis is clear-cut by showing expression levels several thousand times above basal level, protein levels were not proven by Western-blotting because of an lack of specificity of currently available lots of KCa3.1-Ab. Yet, transgene function was verified by patch-clamp electrophysiology showing clear-cut KCa3.1 functions in keratinocyte that far larger than in keratinocyte, in which the channel has not been induced. The skin phenotype characterized by epidermal spongiosis, hyperplasia, hyperkeratosis causing visible skin alterations and itch is solid and reproducible and we provide evidence that this phenotype is caused by channel functions since a selective channel prevents to a considerable extent this phenotype. The changes in the skin cytokine expression profile shows clear increases IL-1β and IL-6, pointing to the contribution of these cytokines to the development of this phenotype. Yet, we are aware of the expectantly high physiological complexity when studying an in-vivo model and, for instance, do not wish to exclude additional systemic mechanisms, e.g. a contribution of the immune system.

Despite these limitations, it is still worth mentioning that compared with human skin diseases, the skin phenotype in KCa3.1+ mice share similarities with human eczematous dermatitis characterized by spongiosis, epidermal hyperplasia, and itch, as important pathological features [43]. Yet, the cellular mechanisms causing this condition and, particularly, spongiosis

are poorly understood. In this regard, it is tempting to speculate that epidermal KCa3.1 could also be a mechanistic player in human skin disease. Yet, at present a pathomechanistic role of KCa3.1 has not been shown for human skin conditions with the exception of role in melanoma cell proliferation. Still, our study provides the rationale to investigate KCa3.1-function in specifically eczematous dermatitis with keratinocyte hyperplasia and in other skin pathologies, characterized by excessive keratinocyte growth such as psoriasis, and test clinical efficacy of KCa3.1-inhibitors.

In conclusion, epidermal KCa3.1 overexpression in murine skin produces itchy eczematous dermatitis. This can be dampened by pharmacological channel inhibition. Future target identification and validation studies in patients will show whether KCa3.1-inhibitors are of therapeutic utility in human skin pathologies.

Supporting information

S1 Data.
(XLSX)

S2 Data.
(XLSX)

S1 Fig.
(PPTX)

S1 Movie. Supplemental Media file 1; Description: Two sequences showing mice treated with DOX for two weeks and a sequence showing control mice receiving only sucrose. Of the last two sequences, the first shows a mouse from the Senicapoc trial that did not receive Senicapoc. The second sequence shows a mouse that received Senicapoc.
(MP4)

Acknowledgments

We thank Andrea Lorda for excellent technical assistance and the scientific staff of the IACS: Dr. Maria Royo (IACS), Dr. Mark Strunk, Alicia de Diego Olmos and the staff of animal of the animal core facility IACS for IHC stains, genotyping, animal breeding and collecting tissue, respectively.

Author Contributions

Conceptualization: Hiroto Miura, Yolanda Gilaberte, Ralf Köhler.

Data curation: Ralf Köhler.

Formal analysis: Javier Lozano-Gerona, Ralf Köhler.

Funding acquisition: Esther Pueyo, Ángel-Luis Garcia-Otín, Pilar Giraldo, Hiroto Miura, Ralf Köhler.

Investigation: Javier Lozano-Gerona, Aida Oliván-Viguera, Pablo Delgado-Wicke, Vikrant Singh, Brandon M. Brown, Elena Tapia-Casellas, Marta Sofía Valero, Ángel-Luis Garcia-Otín, Edgar Abarca-Lachen, Kirk L. Hamilton, Siba P. Raychaudhuri, Miguel Marigil, Ángeles Juarranz, Heike Wulff, Hiroto Miura, Yolanda Gilaberte, Ralf Köhler.

Methodology: Javier Lozano-Gerona, Aida Oliván-Viguera, Pablo Delgado-Wicke, Elena Tapia-Casellas, Esther Pueyo, Marta Sofía Valero, Joaquín C. Surra, Jesús Osada, Siba P. Raychaudhuri, Miguel Marigil, Ángeles Juarranz, Heike Wulff, Hiroto Miura, Ralf Köhler.

Project administration: Ralf Köhler.

Resources: Elena Tapia-Casellas, Esther Pueyo, Marta Sofía Valero, Ángel-Luis Garcia-Otín, Pilar Giraldo, Joaquín C. Surra, Jesús Osada, Miguel Marigil, Ángeles Juarranz, Heike Wulff, Hiroto Miura, Yolanda Gilaberte, Ralf Köhler.

Supervision: Ralf Köhler.

Validation: Ralf Köhler.

Visualization: Javier Lozano-Gerona, Pablo Delgado-Wicke, Elena Tapia-Casellas, Kirk L. Hamilton, Siba P. Raychaudhuri, Miguel Marigil, Ángeles Juarranz, Ralf Köhler.

Writing – original draft: Javier Lozano-Gerona, Kirk L. Hamilton, Heike Wulff, Hiroto Miura, Ralf Köhler.

Writing – review & editing: Javier Lozano-Gerona, Aida Oliván-Viguera, Pablo Delgado-Wicke, Vikrant Singh, Brandon M. Brown, Elena Tapia-Casellas, Esther Pueyo, Marta Sofía Valero, Ángel-Luis Garcia-Otín, Pilar Giraldo, Edgar Abarca-Lachen, Joaquín C. Surra, Jesús Osada, Kirk L. Hamilton, Siba P. Raychaudhuri, Miguel Marigil, Ángeles Juarranz, Heike Wulff, Hiroto Miura, Yolanda Gilaberte, Ralf Köhler.

References

1. Feske S, Wulff H, Skolnik EY. Ion channels in innate and adaptive immunity. Annu Rev Immunol. 2015; 33: 291–353. https://doi.org/10.1146/annurev-immunol-032414-112212 PMID: 25861976
2. Brown BM, Pressley B, Wulff H. KCa3.1 channel modulators as potential therapeutic compounds for glioblastoma. Curr Neuropharmacol. 2017; 16(5): 618–626.
3. Rabjerg M, Oliván-Viguera A, Hansen LK, Jensen L, Sevelsted-Moller L, Walter S, et al. High expression of KCa3.1 in patients with clear cell renal carcinoma predicts high metastatic risk and poor survival. PLoS One. 2015; 10(4): e0122992. https://doi.org/10.1371/journal.pone.0122992 PMID: 25848765
4. Arcangeli A, Becchetti A. Novel perspectives in cancer therapy: Targeting ion channels. Drug Resist Updat. 2015; 21–22: 11–9. https://doi.org/10.1016/j.drup.2015.06.002 PMID: 26183291
5. Oliván-Viguera A, Garcia-Otin AL, Lozano-Gerona J, Abarca-Lachen E, Garcia-Malinis AJ, Hamilton KL, et al. Pharmacological activation of TRPV4 produces immediate cell damage and induction of apoptosis in human melanoma cells and HaCaT keratinocytes. PLoS One. 2018; 13(1): e0190307 https://doi.org/10.1371/journal.pone.0190307 PMID: 29293584
6. Kundu-Raychaudhuri S, Chen YJ, Wulff H, Raychaudhuri SP. Kv1.3 in psoriatic disease: PAP-1, a small molecule inhibitor of Kv1.3 is effective in the SCID mouse psoriasis—xenograft model. J Autoimmun. 2014; 55: 63–72. https://doi.org/10.1016/j.jaut.2014.07.003 PMID: 25175978
7. Oh MH, Oh SY, Lu J, Lou H, Myers AC, Zhu Z, et al. TRPA1-dependent pruritus in IL-13-induced chronic atopic dermatitis. J Immunol. 2013; 191(11):5371–82. https://doi.org/10.4049/jimmunol.1300300 PMID: 24140646
8. Eytan O, Fuchs-Telem D, Mevorach B, Indelman M, Bergman R, Sarig O, et al. Olmsted syndrome caused by a homozygous recessive mutation in TRPV3. J Invest Dermatol. 2014; 134(6):1752–4. https://doi.org/10.1038/jid.2014.37 PMID: 24463422
9. Chen Y, Moore CD, Zhang JY, Hall RP, MacLeod AS, Liedtke W. TRPV4 Moves toward center-fold in Rosacea pathogenesis. J Invest Dermatol. 2017; 137(4): 801–4. https://doi.org/10.1016/j.jid.2016.12.013 PMID: 28340683
10. Moore C, Cevikbas F, Pasolli HA, Chen Y, Kong W, Kempkes C, et al. UVB radiation generates sunburn pain and affects skin by activating epidermal TRPV4 ion channels and triggering endothelin-1 signaling. Proc Natl Acad Sci U S A. 2013; 110(34): E3225–34. https://doi.org/10.1073/pnas.1312933110 PMID: 23929777
11. Caterina MJ, Pang Z. TRP channels in skin biology and pathophysiology. Pharmaceuticals (Basel). 2016; 9(4).
12. Wei AD, Gutman GA, Aldrich R, Chandy KG, Grissmer S, Wulff H. International Union of Pharmacology. LII. Nomenclature and molecular relationships of calcium-activated potassium channels. Pharmacol Rev. 2005; 57(4): 463–72. https://doi.org/10.1124/pr.57.4.9 PMID: 16382103

13. Ishii TM, Silvia C, Hirschberg B, Bond CT, Adelman JP, Maylie J. A human intermediate conductance calcium-activated potassium channel. Proc Natl Acad Sci U S A. 1997; 94(21): 11651–6. https://doi.org/10.1073/pnas.94.21.11651 PMID: 9326665

14. Lee CH, MacKinnon R. Activation mechanism of a human SK-calmodulin channel complex elucidated by cryo-EM structures. Science. 2018; 360(6388): 508–13. https://doi.org/10.1126/science.aas9466 PMID: 29724949

15. Vandorpe DH, Shmukler BE, Jiang L, Lim B, Maylie J, Adelman JP, et al. cDNA cloning and functional characterization of the mouse Ca^{2+}-gated K^+ channel, mIK1. Roles in regulatory volume decrease and erythroid differentiation. J Biol Chem. 1998; 273(34): 21542–53. https://doi.org/10.1074/jbc.273.34.21542 PMID: 9705284

16. Grgic I, Kaistha BP, Paschen S, Kaistha A, Busch C, Si H, et al. Disruption of the Gardos channel (KCa3.1) in mice causes subtle erythrocyte macrocytosis and progressive splenomegaly. Pflugers Arch. 2009; 458(2): 291–302. https://doi.org/10.1007/s00424-008-0619-x PMID: 19037656

17. Wulff H, Miller MJ, Hansel W, Grissmer S, Cahalan MD, Chandy KG. Design of a potent and selective inhibitor of the intermediate-conductance Ca^{2+}-activated K^+ channel, IKCa1: a potential immunosuppressant. Proc Natl Acad Sci U S A. 2000; 97(14): 8151–6. https://doi.org/10.1073/pnas.97.14.8151 PMID: 10884437

18. Toyama K, Wulff H, Chandy KG, Azam P, Raman G, Saito T, et al. The intermediate-conductance calcium-activated potassium channel KCa3.1 contributes to atherogenesis in mice and humans. J Clin Invest. 2008; 118(9): 3025–37. https://doi.org/10.1172/JCI30836 PMID: 18688283

19. Chen YJ, Nguyen HM, Maezawa I, Grössinger EM, Garing AL, Köhler R, et al. The potassium channel KCa3.1 constitutes a pharmacological target for neuroinflammation associated with ischemia/reperfusion stroke. J Cereb Blood Flow Metab. 2016; 36(12): 2146–61. https://doi.org/10.1177/0271678X15611434 PMID: 26661208

20. Devor DC, Singh AK, Frizzell RA, Bridges RJ. Modulation of Cl^- secretion by benzimidazolones. I. Direct activation of a Ca^{2+}-dependent K^+ channel. Am J Physiol. 1996; 271(5 Pt 1):L775–84.

21. Bertuccio CA, Lee SL, Wu G, Butterworth MB, Hamilton KL, Devor DC. Anterograde trafficking of KCa3.1 in polarized epithelia is Rab1- and Rab8-dependent and recycling endosome-independent. PLoS One. 2014; 9(3): e92013. https://doi.org/10.1371/journal.pone.0092013 PMID: 24632741

22. Si H, Heyken WT, Wölfle SE, Tysiac M, Schubert R, Grgic I, et al. Impaired endothelium-derived hyperpolarizing factor-mediated dilations and increased blood pressure in mice deficient of the intermediate-conductance Ca^{2+}-activated K^+ channel. Circ Res. 2006; 99(5): 537–44. https://doi.org/10.1161/01.RES.0000238377.08219.0c PMID: 16873714

23. Wulff H, Köhler R. Endothelial small-conductance and intermediate-conductance KCa channels: an update on their pharmacology and usefulness as cardiovascular targets. J Cardiovasc Pharmacol. 2013; 61(2): 102–12. https://doi.org/10.1097/FJC.0b013e318279ba20 PMID: 23107876

24. Köhler R, Oliván-Viguera A, Wulff H. Endothelial small- and intermediate-conductance K channels and endothelium-dependent hyperpolarization as drug targets in cardiovascular disease. Adv Pharmacol. 2016; 77: 65–104. https://doi.org/10.1016/bs.apha.2016.04.002 PMID: 27451095

25. Albaqumi M, Srivastava S, Li Z, Zhdnova O, Wulff H, Itani O, et al. KCa3.1 potassium channels are critical for cAMP-dependent chloride secretion and cyst growth in autosomal-dominant polycystic kidney disease. Kidney Int. 2008; 74(6): 740–9. https://doi.org/10.1038/ki.2008.246 PMID: 18547995

26. Grgic I, Kiss E, Kaistha BP, Busch C, Kloss M, Sautter J, et al. Renal fibrosis is attenuated by targeted disruption of KCa3.1 potassium channels. Proc Natl Acad Sci U S A. 2009; 106(34): 14518–23. https://doi.org/10.1073/pnas.0903458106 PMID: 19706538

27. Hua X, Deuse T, Chen YJ, Wulff H, Stubbendorff M, Köhler R, et al. The potassium channel KCa3.1 as new therapeutic target for the prevention of obliterative airway disease. Transplantation. 2013; 95(2): 285–92. https://doi.org/10.1097/TP.0b013e318275a2f4 PMID: 23325003

28. Roach KM, Wulff H, Feghali-Bostwick C, Amrani Y, Bradding P. Increased constitutive inverted question markSMA and Smad2/3 expression in idiopathic pulmonary fibrosis myofibroblasts is KCa3.1-dependent. Respir Res. 2014; 15(1): 155.

29. Huang C, Pollock CA, Chen XM. Role of the potassium channel KCa3.1 in diabetic nephropathy. Clin Sci (Lond). 2014; 127(7): 423–33.

30. Zhao LM, Wang LP, Wang HF, Ma XZ, Zhou DX, Deng XL. The role of KCa3.1 channels in cardiac fibrosis induced by pressure overload in rats. Pflugers Arch. 2015; 467(11): 2275–85. https://doi.org/10.1007/s00424-015-1694-4 PMID: 25715999

31. Köhler R, Wulff H, Eichler I, Kneifel M, Neumann D, Knorr A, et al. Blockade of the intermediate-conductance calcium-activated potassium channel as a new therapeutic strategy for restenosis. Circulation. 2003; 108(9): 1119–25. https://doi.org/10.1161/01.CIR.0000086464.04719.DD PMID: 12939222

32. Tharp DL, Wamhoff BR, Wulff H, Raman G, Cheong A, Bowles DK. Local delivery of the KCa3.1 blocker, TRAM-34, prevents acute angioplasty-induced coronary smooth muscle phenotypic modulation and limits stenosis. Arterioscler Thromb Vasc Biol. 2008; 28(6): 1084–9. https://doi.org/10.1161/ATVBAHA.107.155796 PMID: 18309114

33. D'Alessandro G, Catalano M, Sciaccaluga M, Chece G, Cipriani R, Rosito M, et al. KCa3.1 channels are involved in the infiltrative behavior of glioblastoma in vivo. Cell Death Dis. 2013; 4: e773. https://doi.org/10.1038/cddis.2013.279 PMID: 23949222

34. Jiang S, Zhu L, Yang J, Hu L, Gu J, Xing X, et al. Integrated expression profiling of potassium channels identifies KCNN4 as a prognostic biomarker of pancreatic cancer. Biochem Biophys Res Commun. 2017; 494(1–2): 113–9. https://doi.org/10.1016/j.bbrc.2017.10.072 PMID: 29050937

35. Wulff H, Castle NA. Therapeutic potential of KCa3.1 blockers: recent advances and promising trends. Expert Rev Clin Pharmacol. 2010; 3(3): 385–96. https://doi.org/10.1586/ecp.10.11 PMID: 22111618

36. Christophersen P, Wulff H. Pharmacological gating modulation of small- and intermediate-conductance Ca2+-activated K+ channels (KCa2.x and KCa3.1). Channels (Austin). 2015; 9(6): 336–43.

37. Ataga KI, Reid M, Ballas SK, Yasin Z, Bigelow C, James LS, et al. Improvements in haemolysis and indicators of erythrocyte survival do not correlate with acute vaso-occlusive crises in patients with sickle cell disease: a phase III randomized, placebo-controlled, double-blind study of the Gardos channel blocker senicapoc (ICA-17043). Br J Haematol. 2011; 153(1): 92–104. https://doi.org/10.1111/j.1365-2141.2010.08520.x PMID: 21323872

38. Maezawa I, Jenkins DP, Jin BE, Wulff H. Microglial KCa3.1 channels as a potential therapeutic target for Alzheimer's disease. Int J Alzheimers Dis. 2012; 2012: 868972. https://doi.org/10.1155/2012/868972 PMID: 22675649

39. Thompson-Vest N, Shimizu Y, Hunne B, Furness JB. The distribution of intermediate-conductance, calcium-activated, potassium (IK) channels in epithelial cells. J Anat. 2006; 208(2): 219–29. https://doi.org/10.1111/j.1469-7580.2006.00515.x PMID: 16441566

40. Hochedlinger K, Yamada Y, Beard C, Jaenisch R. Ectopic expression of Oct-4 blocks progenitor-cell differentiation and causes dysplasia in epithelial tissues. Cell. 2005; 121(3): 465–77. https://doi.org/10.1016/j.cell.2005.02.018 PMID: 15882627

41. Jin LW, Lucente JD, Nguyen HM, Singh V, Singh L, Chavez M, et al. Repurposing the KCa3.1 inhibitor senicapoc for Alzheimer's disease. Ann Clin Transl Neurol. 2019; 6(4): 723–738. https://doi.org/10.1002/acn3.754 PMID: 31019997

42. Oliván-Viguera A, Valero MS, Coleman N, Brown BM, Laria C, Murillo MD, et al. A novel pan-negative-gating modulator of KCa2/3 channels, the fluoro-di-benzoate, RA-2, inhibits EDH-type relaxation in coronary artery and produces bradycardia in vivo. Mol Pharmacol. 2015; 87: 1–12. https://doi.org/10.1124/mol.114.095661

43. Nedorost ST. Generalized dermatitis in clinical practice: Springer: Science & Business Media; 2012. pp. 1–3, 9, 13–4 p.

44. Seeger MA, Paller AS. The roles of growth factors in keratinocyte migration. Adv Wound Care (New Rochelle). 2015; 4(4): 213–24.

45. Sevelsted-Moller L, Fialla AD, Schierwagen R, Biagini M, Reul W, Klein S, et al. KCa3.1 channels are up-regulated in hepatocytes of cirrhotic patients. J Hepatol. 2015; 62: S481.

46. Valero MS, Ramón-Gimenez M, Lozano-Gerona J, Delgado-Wicke P, Calmarza P, Oliván-Viguera A, et al. KCa3.1 Transgene induction in murine intestinal epithelium causes duodenal chyme accumulation and impairs duodenal contractility. Int J Mol Sci. 2019 Mar 8; 20(5): E1193. https://doi.org/10.3390/ijms20051193 PMID: 30857243

47. Di L, Srivastava S, Zhdanova O, Ding Y, Li Z, Wulff H, et al. Inhibition of the K^+ channel KCa3.1 ameliorates T cell-mediated colitis. Proc Natl Acad Sci U S A. 2010; 107(4): 1541–6. https://doi.org/10.1073/pnas.0910133107 PMID: 20080610

48. Koch Hansen L, Sevelsted-Moller L, Rabjerg M, Larsen D, Hansen TP, Klinge L, et al. Expression of T-cell KV1.3 potassium channel correlates with pro-inflammatory cytokines and disease activity in ulcerative colitis. J Crohns Colitis. 2014; 8(11): 1378–91. https://doi.org/10.1016/j.crohns.2014.04.003 PMID: 24793818